Journal of Teikyo Heisei University Vol.21 No.1

帝京平成大学紀要 第21巻 第1号

Freshwater Crabs from Surat Thani, Peninsular Thailand, as Intermediate Hosts of Lung Flukes

TAKEDA Masatsune, SUGIYAMA Hiromu

and RANGSIRUJI Achariya

Journal of Teikyo Heisei University
Vol.21 No.1

March 2010

Campus Ikebukuro

Journal of Teikyo Heisei University Vol. 21 No. 1

帝京平成大学紀要 第21巻 第1号

Freshwater Crabs from Surat Thani, Peninsular Thailand, as Intermediate Hosts of Lung Flukes

TAKEDA Masatsune[1], SUGIYAMA Hiromu[2] and RANGSIRUJI Achariya[3]

肺吸虫の中間宿主としてのタイ南部スラタニ産淡水カニ類

武田正倫[1]・杉山　広[2]・アチャリア ラングシルジ[3]

摘　要

タイ南部のスラタニ産3種のサワガニ類（2科3属）から肺吸虫のメタセルカリア幼虫が検出されたが、サワガニ類の同定は容易でないことから、本論文において写真により識別形質を明示した。3種はGecarcinucidae科の *Phricotelphusa aedes* (Kemp, 1923) と *Thaksinthelphusa yongschiandaratae* (Naiyanetr, 1988) およびPotamidae サワガニ科の *Demanietta renongensis* (Rathbun, 1905) である。なお、肺吸虫の幼虫は検出されなかったが、同地域から採集されたParathelphusidae科の *Sayamia germaini* (Rathbun, 1902) と *Siamthelphusa improvisa* (Lancheter, 1901) も参考までに記録した。

Abstract

Three freshwater crabs from Surat Thani Province, peninsular Thailand proved to be the intermediate hosts of lung flukes are recorded, with some fine photographs, to facilitate their identification. They are *Phricotelphusa aedes* (Kemp, 1923) and *Thaksinthelphusa yongschiandaratae* (Naiyanetr, 1988) of the family Gecarcinucidae, and *Demanietta renongensis* (Rathbun, 1905) of the family Potamidae. In addition to them, *Sayamia germaini* (Rathbun, 1902) and *Siamthelphusa improvisa* (Lanchester, 1901) of the family Parathelphsidae collected from the same area during the field survey are recorded, although they are negative to parasite infection.

Keywords: Freshwater crab, *Phricotelphusa aedes*, *Thaksinthelphusa yongschiandaratae*, *Demanietta renongensis*, *Sayamia germaini*, *Siamthelphusa improvisa*, Gecarcinucidae, Parathelphusidae, Potamidae, Surat Thani, Thailand

---

1) Corresponding author. Faculty of Modern Life, Teikyo Heisei University, 2-51-4 Higashi-Ikebukuro,Toshima-ku, Tokyo, 170-8445 Japan; e-mail takeda-m@thu.ac.jp
東京都豊島区東池袋2-51-4 帝京平成大学 現代ライフ学部

2) Department of Parasitology, National Institute of Infectious Diseases, Tokyo, Japan
国立感染症研究所 寄生動物部

3) Department of Biology, Faculty of Science, Srinakharinwirot University, Bangkok, Thailand
シーナカリンウィロート大学 理学部 生物学教室

Introduction

The junior authors, H. Sugiyama and A. Rangsiruji, have been engaged in field research of the lung flukes from Thailand for several years, and collected many specimens of freshwater crabs that may become the second intermediate host. Occurrence of some larval cysts of the parasites has been already reported (Rangsiruji *et al.*, 2006[1]; Sugiyama *et al.*, 2007[2]).

Many species of Thai freshwater crabs have been described by Prof. Phaibul Naiyanetr of Chulalongkorn University, Bangkok, and then some nomenclaturally revised and supplemental papers were published with aid of Dr. Peter K. L. Ng of the University of Singapore. It is, however, still not easy to identify Thai freshwater crabs mainly because of the remarkable diversity in various niches such as leaf litter, paddy field, waterfall, mountain stream, and others. In this paper two species of the family Gecarcinucidae and one species of the family Potamidae harboring the larval cysts of lung flukes from Surat Thani, peninsular Thailand are explained taxonomically, with some photographs of the distinguishing characters useful for subsequent identification. In addition to them, two species of the family Parathelphusidae from the same area are recorded, although they are negative to parasite infection.

The specimens examined are preserved in the National Museum of Nature and Science, Tokyo, Japan. In this paper the measurements were made only for the carapace with caliper in mm, using the abbreviations of cb (carapace breadth) and cl (carapace length).

Family Gecarcinucidae

Genus ***Phricotelphusa*** Alcock, 1909

Phricotelphusa aedes (Kemp, 1923)

(Figs. 1 A, 2 A, 3)

Paratelphusa (Phricotelphusa) aedes Kemp, 1923[3], p. 39, pl. 4 fig. 12.

Phricotelphusa aedes - Naiyanetr, 1998[4], p. 195 (in list), 1 color photo.

Material examined. Phanom District, Surat Thani. — Jan.-Feb. 2003, 3 ♂♂ (cb 21.6 × cl 16.4 mm; cb 17.7 × cl 13.7 mm; cb 11.2 × cl 10.0 mm) 2 ♀♀ (cb 21.2 × cl 16.3 mm; cb 15.7 × cl 12.2 mm); May 2003, 1 ♂ (cb 13.7 × cl 11.5 mm), 1 ♀ (partly damaged).

Remarks. Bott (1970)[5] definitely synonymized this species with *Phricotelphusa limula* (Hilgendorf, 1882)[6] based on the examination of the type specimen. The fortified argument was not given, only with its identity, but later Prof. Naiyanetr, who identified the present specimens, was of opinion that both species are valid, and thus Ng (1986)[7] compared his new species, *P. hockpingi* from west Malaysia, with the topotypic specimens of *P. limula* from Phuket Island. At present, although it seems to be difficult to find the distinct differences between these two species without direct comparison, the identification was followed the opinion of Prof. Naiyanetr.

The carapace is oval rather than squarish, with dorsally and laterally convex branchial regions, and its dorsal surface is smooth for its most part, but covered with oblique short costae on the branchial regions (Fig. 2 A); the epigastric and postorbital cristae are distinct and distinctly linear; the epigastric and postorbital cristae are usually isolated from each other by a shallow dorsal depression, but in some specimens the isolation is incomplete, only with a small interruption; the postorbital crista is distinctly separated from the epibranchial tooth by an oblique submarginal furrow running from the hepatic region to the branchial dorsal surface. The epibranchial tooth is rather close to the external orbital angle, small but distinct, directed obliquely forward and upward. The male and female abdomens are as in the photographs. The first male pleopod is rather short, weakly curved outward, tapering toward small terminal aperture; the terminal segment is about one third as long as the shaft. The second male pleopod is long, with

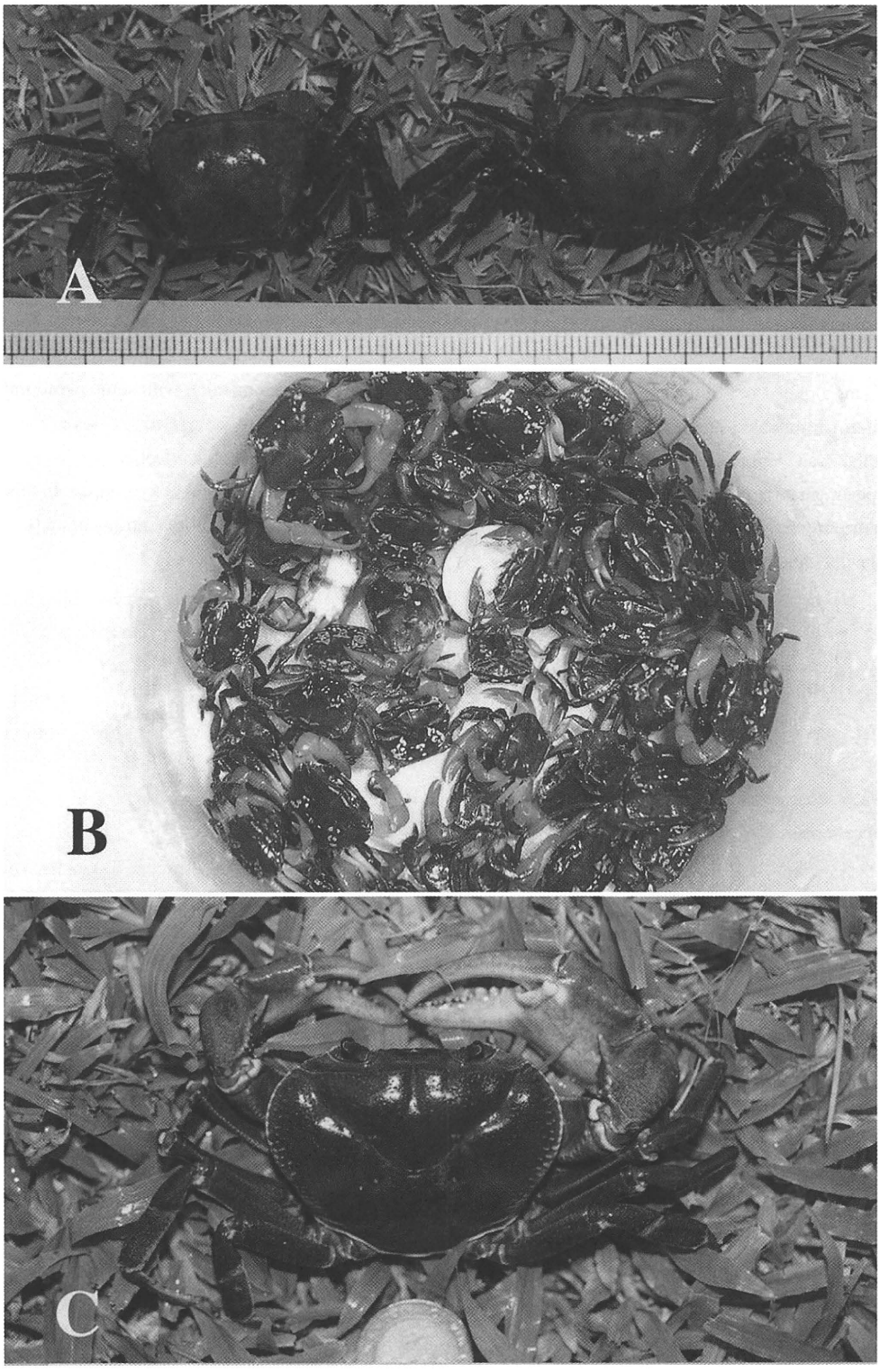

Fig. 1. A, *Phricotelphusa aedes* (Kemp), female (left) and male (right); B, *Thaksinthelphusa yongschiandaratae* (Naiyanetr), specimens in a bucket; C, *Demanietta renongensis* (Rathbun), male.

the flagellum almost two thirds as long as the basal portion; the flagellum is grooved and subtruncated at its tip.

Note. Metacercariae of *Paragonimus westermani* (Kerbert, 1878) and *P. bangkokensis* Miyazaki & Vajrasthira, 1967, and also metacercariae of *P. westermani*-like were isolated (Sugiyama *et al.*, 2007)[2].

Distribution. Previously known only from Nahkon Si Thammarat Province, peninsular Thailand.

Genus ***Thaksinthelphusa*** Ng & Naiyanetr, 1993

Thaksinthelphusa yongschiandaratae (Naiyanetr, 1988)

(Figs. 1B, 2B, 4)

Phricotelphusa yongschiandaratae Naiyanetr, 1988a[8], p. 99; 1988b[9], p. 10, pl. 7 fig. 5.

Thaksinthelphusa yongschiandaratae – Ng & Naiyanetr, 1993[10], p. 36, figs. 25, 60.

Material examined. Phanom District, Surat Thani. — Jan.-Feb. 2003, 1 ovig. ♀ (cb16.3 × cl12.0mm); Feb. 2008, 2 ♂♂ (cb21.4 × cl14.7mm; cb 18.9 × cl13.5mm) and 2 ♀♀ (cb18.8 × cl13.7mm; cb 16.9 × cl12.2mm).

Remarks. This species is the monotypical representative of the genus *Thaksinthelphusa*, without problem in its identification due to the important contribution of Ng & Naiyanetr (1993)[10] who recorded the accurate name of the type locality instead of incorrect record in the original description.

This species is small in size, and most characteristic in the features that the epigastric and postorbital cristae are fused as a long transverse ridge without interruption (Fig. 2B), and the ischium of the third maxilliped is entirely smooth without median sulcus (Figs. 4A, C). The contour of the carapace is rather rectangular, and its dorsal surface is flattened as a whole, sunken to form a transverse groove in front of, and flattened for its most part behind the epigastric-postorbital crests of both sides. The male abdomen is narrow, with the lateral margins of the weakly concave terminal and weakly convex subterminal segments (Fig. 4B).

Note. Metacercariae of *Paragonimus westermani* (Kerbert, 1878) and *P. bangkokensis* Miyazaki & Vajrasthira, 1967 were isolated.

Distribution. Previously known only from the type locality, Bang Phrik Waterfall, Amphoe Takua Pa, Phangnga Province, peninsular Thailand.

Family Potamidae

Genus ***Demanietta*** Bott, 1966

Demanietta renongensis (Rathbun, 1905)

(Figs. 1C, 2C, 5)

Potamon (Potamonautes) renongensis Rathbun, 1905[11], p. 176.

Potamiscus (Demanietta) tenasserimensis smalleyi Bott, 1966[12], p. 490, fig. 25, pl. 19 fig. 8.

Ranguna (Demanietta) tenaerimensis smalleyi - Bott, 1970[5], p. 175, pl. 39 fig. 49, pl. 50 fig. 45.

Demanietta smalleyi - Naiyanetr, 1998[4], p. 109 (in list), 1 color photo.

Demanietta renongensis - Yeo *et al.*, 1999[13], p. 536, figs. 2G-N, 6C, D, 8B, 9B.

Material examined. Phanom District, Surat Thani. — Jan.-Feb. 2003, 1 ♀ (cb33.5 × cl25.0mm), 1 ♂ (cb 37.2 × cl27.8mm); May 2003, 2 ♂♂ (cb62.0 × cl43.8mm; cb49.2 × cl35.4mm), 1 ♀ (cb41.6 × cl33.7mm).

Remarks. This large species hitherto known under some different names was definitely referred to the genus *Demanietta*, the systematic status of which has been fully discussed and re-established by Yeo *et al.* (1999)[13]. The representative species are at present 10 known from both sides of the Tenasserim Range bordering Thailand and Myanmar, central and southeastern Thai provinces, and some islands and the Mergui Archipelago in the eastern

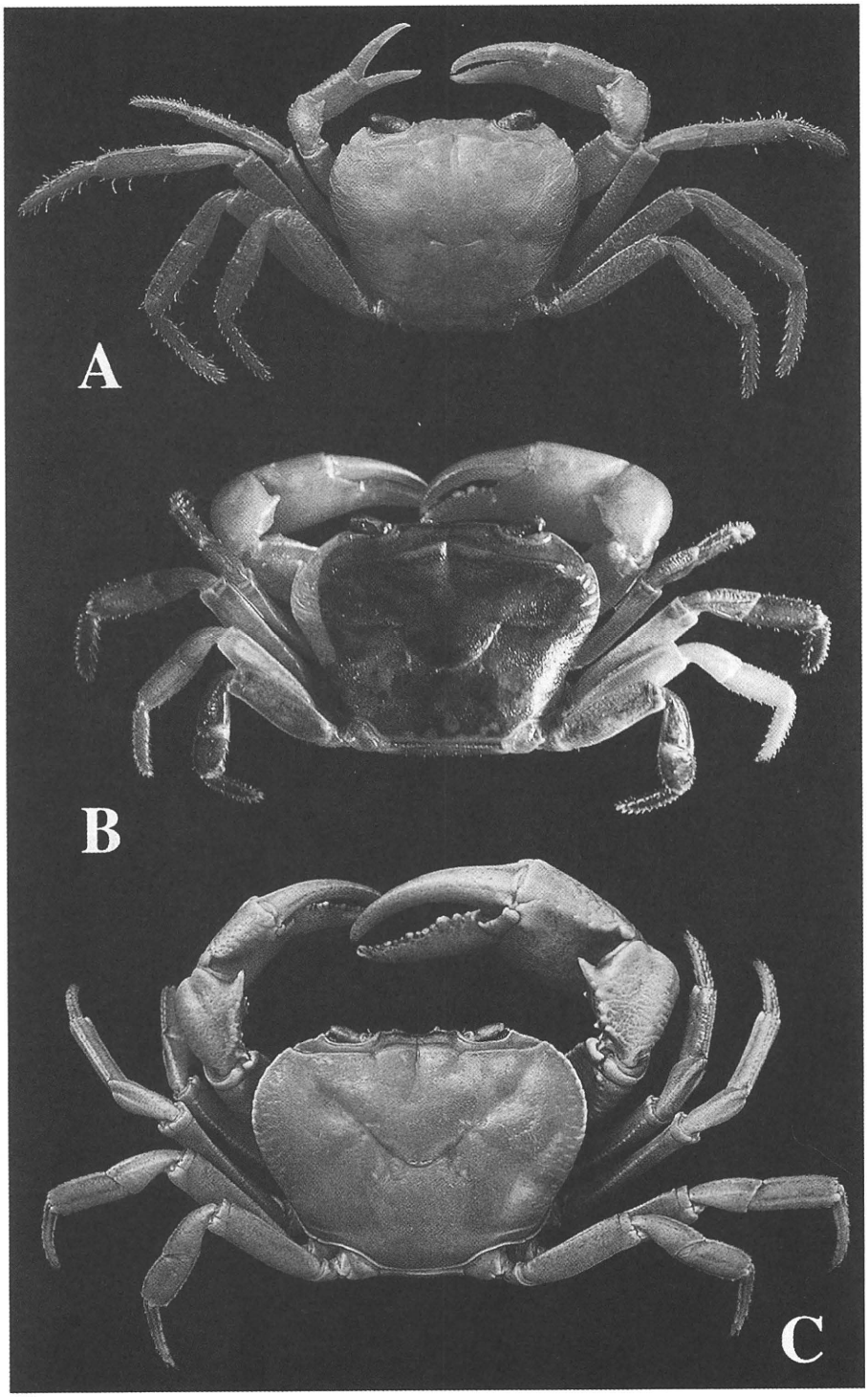

Fig. 2. A, *Phricotelphusa aedes* (Kemp), male (cb 21.6 × cl 16.4 mm); B, *Thaksinthelphusa yongschiandaratae* (Naiyanetr), male (cb 21.4 × cl 14.7 mm); C, *Demanietta renongensis* (Rathbun), male (cb 62.0 × cl 43.8 mm).

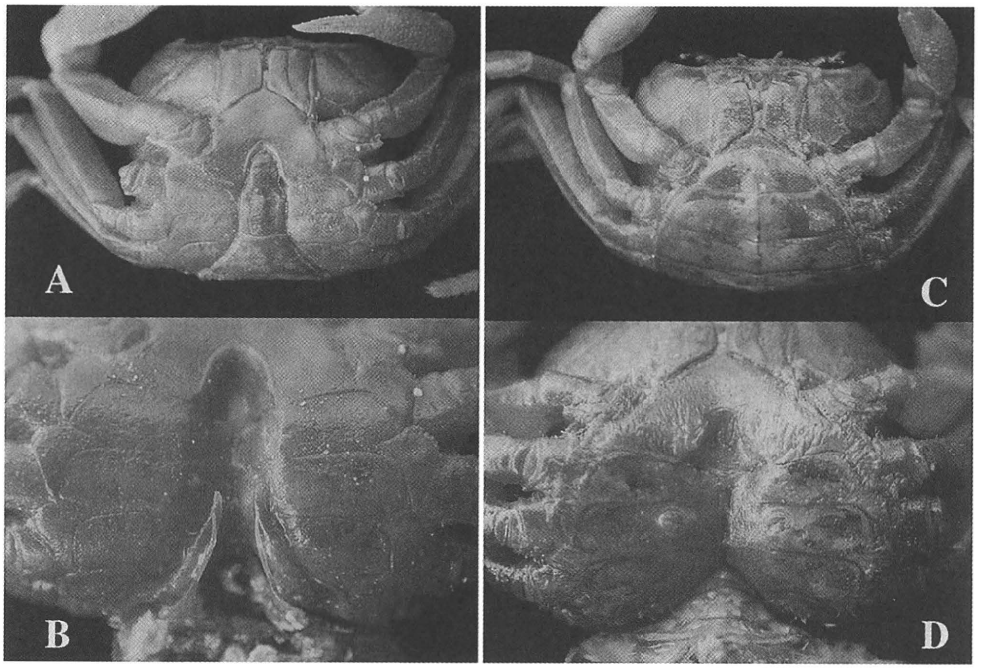

Fig. 3. *Phricotelphusa aedes* (Kemp). A, B, male (cb 21.6 × cl 16.4 mm); C, D, female (cb 18.8 × cl 13.7 mm).

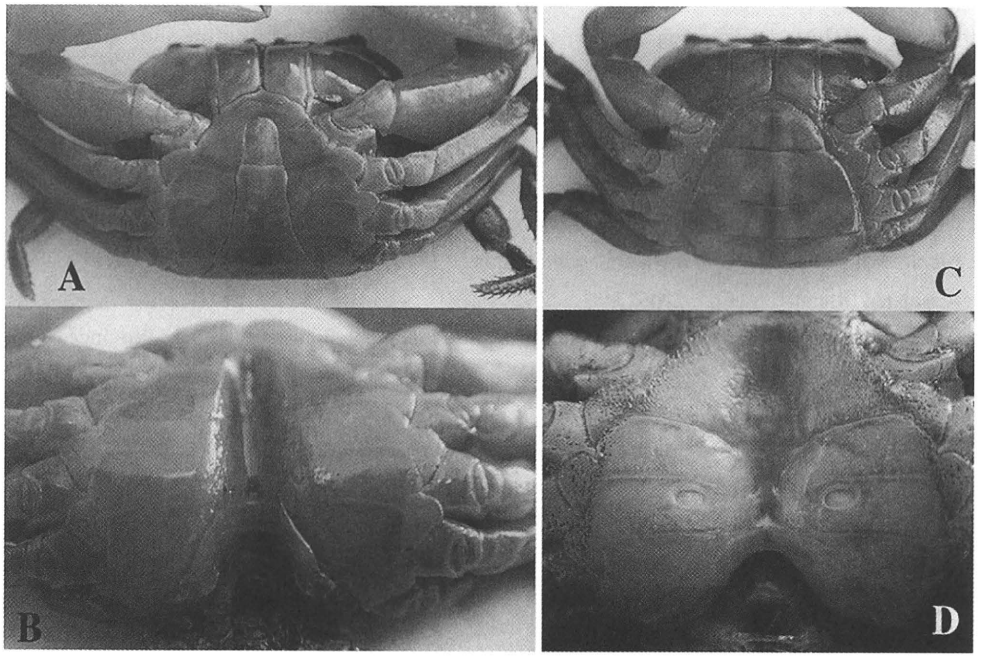

Fig. 4. *Thaksinthelphusa yongschiandaratae* (Naiyanetr). A, B, male (cb 21.4 × cl 14.7 mm); C, D, female (cb 18.8 × cl 13.7 mm).

Andaman Sea.

The carapace is transversely elliptical, rather flattened on its dorsal surface with submarginal short costae, strong

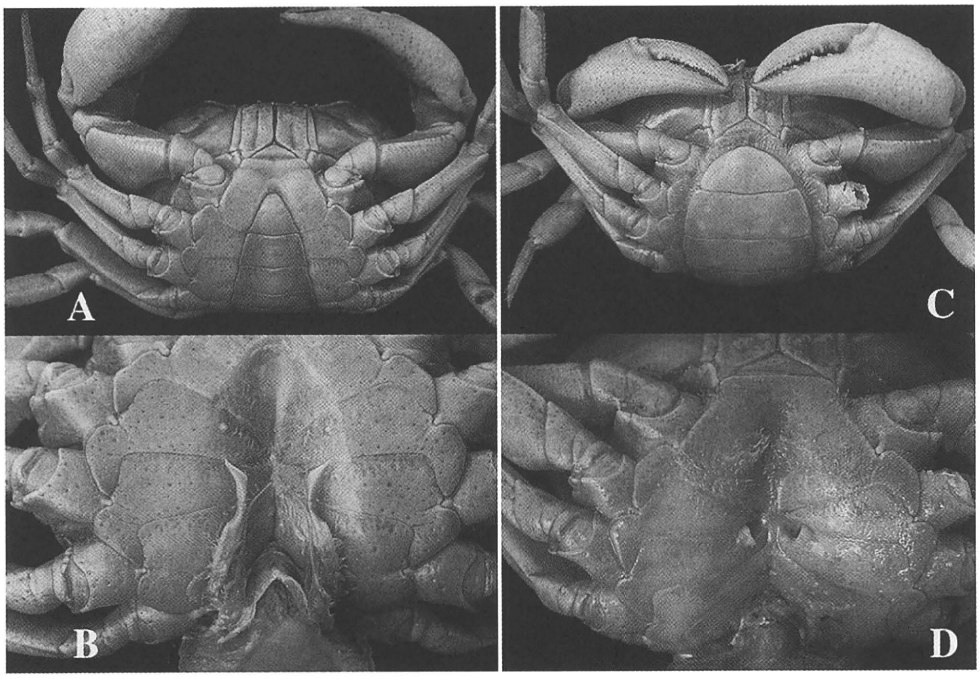

Fig. 5. *Demanietta renongensis* (Rathbun). A, B, male (cb 62.0 × cl 43.8 mm); C, D, female (cb 41.6 × cl 33.7 mm).

epigastric and postorbital cristae; epigastric crista is thick, transverse, slightly before and half as wide as, the postorbital ridge; the gastro-branchial and gastro-cardiac groove are shallow, but prominent, forming a wide V on the dorsal main surface of the carapace. The male abdomen is rather wide and pagoda-shaped; the male first pleopod is stout at its basal half, straight distally, with prominent terminal segment, and the distal half of the terminal segment is curved obliquely outward for its main part and directed forward at tip. In the fully grown male the chelipeds are quite different in size.

Note. Metacercariae of *Paragonimus westermani* (Kerbert, 1878) and *P. bangkokensis* Miyazaki & Vajrasthira, 1967 were isolated (Rangsiruji *et al.*, 2006[1]).

Distribution. Previously known from Chumphon, Ranong, Phangnga, Phuket and Krabi Provinces, peninsular Thailand (Naiyanetr, 1998)[4].

Two Species Negative to Infection of Lung Flukes

In addition to three species of the families Gecarcinucidae and Potamidae from Surat Thani recorded above as inter-mediate hosts of lung flukes, some specimens referable to *Sayamia germaini* (Rathbun, 1902)[14] and *Siamthelphusa improvisa* (Lanchester, 1901)[15] of the family Parathelphusidae were collected from the same localities.

The former species, *Sayamia germaini* known previously as a species of the genus *Somanniathelphusa*, was transferred to the genus *Sayamia* by Naiyanetr (1994)[16]. The genus *Sayamia* contains five Thai-Malayan species, with the type species, *Somanniathelphusa bangkokensis* Naiyanetr, 1982 by the original designation. The record of *Potamon (Parathelphusa) germaini* Rathbun as the type species of *Sayamia* by Ng *et al.* (2008)[17] may be trivial error or of certain reason.

The following is the diagnostic characters of the female examined (Fig. 6A; cb 46.4 × cl 37.8 mm). The carapace

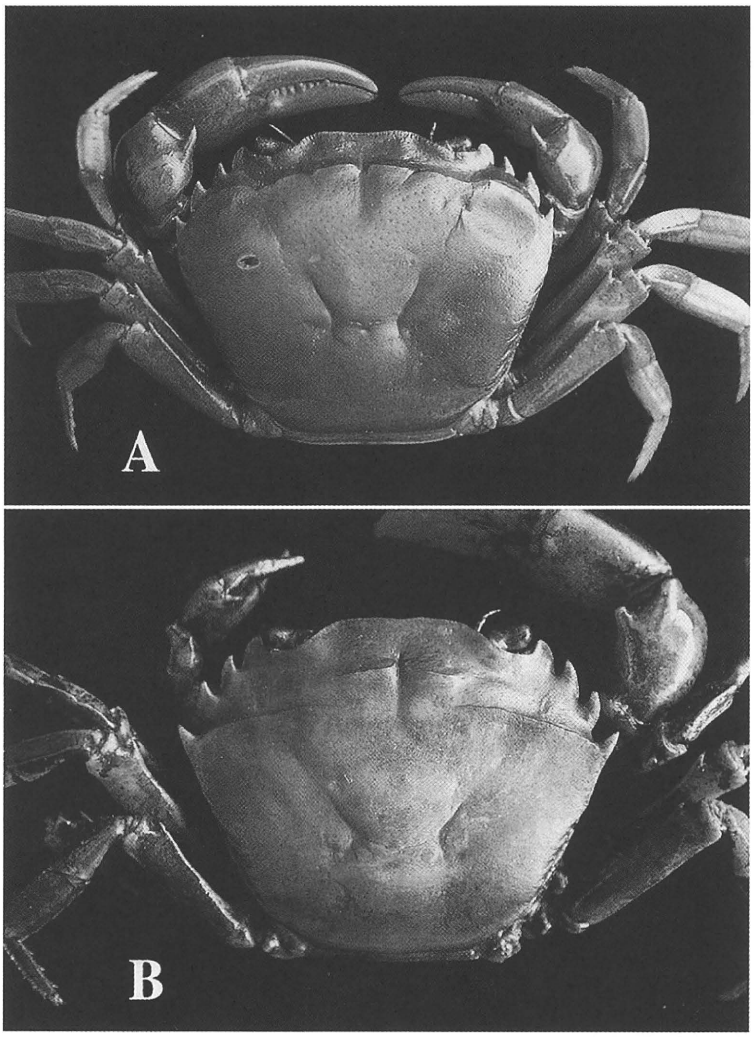

Fig. 6. A, *Sayamia germaini* (Rathbun), female (cb 46.4 × cl 37.8 mm); *Siamthelphusa improvisa* (Lanchester), male (cb 33.4 × cl 26.1 mm).

is strongly convex dorsally, smooth and shining to the naked eye; the epigastric and postorbital cristae are distinct and isolated from each other by a shallow interruption; the inner half of the postorbital crista is sinuous, and concave posteriorly behind the outer part of the orbit; the outer half is convex obliquely forward and then running to the last epibranchial tooth without interruption. The external orbital tooth is flattened and lobular, with the blunt apex and the convex outer margin. The anterolateral margin of the carapace is armed with three sharp epibranchial teeth; the first and third are subequal, but the former is more strongly curved obliquely inward and the latter nearly forward; the second is similar to the first in shape, but larger.

According to Naiyanetr (1998)[4], *Sayamia germaini* is widely distributed in central, west, east and south Thailand. In peninsular Thailand, it is known from Ranong, Surat Thani, Nakhon Si Thammarat and Songkhla Provinces.

In the collections at hand, *Siamthelphusa improvisa* is represented only by a male (Fig. 6B; cb 33.4 × cl 26.1 mm). This is one of nine species of the genus *Siamthelphusa* from northern peninsular Malaysia and Thailand distinguished by Ng and Naiyanetr (1997)[18] who made the useful diagnoses and key, with fine figures. Earlier than

their paper, Ng and Lim (1986)[19] made the line drawings of the carapace, chela, male abdomen, first and second male pleopods for the comparison with their new species, *S. insolita* from peninsular Malaysia. Diagnostic characters are given as follows. The dorsal surface of the carapace is flat, with the sharp epigastric and postorbital cristae; the external orbital tooth is flattened and lobular, with the convex outer margin the anterolateral margin is armed with three sharp teeth; the first two teeth are similar in shape and size, weakly curved and directed forward; the third tooth is subequal to, or slightly smaller than the preceding two teeth, straight and directed obliquely outward. The chelipeds are distinctly unequal, and the outer surface of the right (larger) palm is ornamented with dark reticulate pattern.

According to Naiyanetr (1998)[4], *Siamthelphusa improvisa* is known from Nakhon Si Thammarat, Phatthahung and Surat Thani Provinces, peninsular Thailand.

Acknowledgements

For the identification of some specimens and in getting the literature of Thai freshwater crabs, the authors are thankful Prof. Phaibul Naiyanetr of Chulalongkorn University, Bangkok, who is the pioneer and leading carcinologist in Thailand. This study was supported in part by a grant from the Nissan Science Foundation and by grants for Research on Emerging and Re-emerging Infectious Diseases from the Ministry of Health, Labor and Welfare of Japan (H18-Shinko-ippan-008 and H21-Shinko-ippan-004).

Literature

1) Rangsiruji, A., H. Sugiyama, Y. Morishima, Y. Kameoka, T. Donsakul, S. Binchai & P. Ketudat, 2006. A new record of *Paragonimus* other than *P. westermani* in southern Thailand. *SE Asian J. Trop. Med. Public Health*, **37** (Suppl. 3): 57-61.

2) Sugiyama, H., Y. Morishima, S. Binchai, A. Rangsiruji & P. Ketudat, 2007. New form of *Paragonimus westermani* discovered in Thailand: Morphological characteristics and host susceptibility. *SE Asian J. Trop. Med. Public Health*, **38** (Suppl. 1): 87-91.

3) Kemp, S., 1923. On a collection of river crabs from Siam and Annam. *J. Nat. Hist. Soc. Siam*, **6**: 1-42.

4) Naiyanetr, P., 1998. *Checklist of Crustacean Fauna in Thailand (Decapoda and Stomatopoda)*. Office of Environmental Policy and Planning, Bangkok, Thailand, 161 pp.

5) Bott, R., 1970. Die Süsswasserkrabben von Europoa, Asien, Australien und ihre Stammesgeschichite. Eine Revision der Potamoidea und Parathelphusoidea (Crustacea, Decapoda). *Abh. Senck. Nat. Ges.*, (526): 1-338.

6) Hilgendorf, F., 1882. Einige carcinologische Mittheilungen. *S. B. Ges. Nat. Freunde Berlin*, **1882**: 22-25.

7) Ng, P. K. L., 1986. *Phricotelphusa hockpingi* sp. nov., a new gecarcinucid freshwater crab from Perak, west Malaysia (Decapoda, Brachyura). *Crustaceana*, **51**: 270-276.

8) Naiyanetr, P., 1988a. New freshwater crab of Thailand: 2. Proc. 26th Conf. Fish. Sec., Kasetsart Univ., Bangkok, Thailand. (Not directly cited)

9) Naiyanetr, P., 1988b. Fresh water crabs in Thailand. In: Book published in memory of the Royal Cremation of Associate Professor Dr. Praphun Chitachumnong: 15 pp., 8 color pls., Mahidol Univ., Phaisalsipa Press, Bangkok, Thailand. (Not directly cited)

10) Ng, P. K. L. & P. Naiyanetr, 1993. New and recently described freshwater crabs (Crustacea: Decapoda: Brachyura: Potamidae, Gecarcinucidae and Parathelphusidae) from Thailand. *Zool. Verh.*, (284): 1-117.

11) Rathbun, M. J., 1905. Les crabes d'eau douce. *Nouv. Arch. Mus. Hist. Nat.*, Paris, (4), **7**: 159-323.

12) Bott, R., 1966. Potamiden aus Asien (*Potamon* Savigny und *Potamiscus* Alcock) (Crustacea, Decapoda). *Senck.*

Biol., **47**: 469-509

13) Yeo, D. C. J., P. Naiyanetr & P. K. L. Ng, 1999. Revision of the waterfall crabs of the genus *Demanietta* (Decapoda: Brachyura: Potamidae). *J. Crust. Biol.*, **19**: 530-555.

14) Rathbun, M. J., 1902. Description des nouvelles espèces de *Parathelphusa* appartenant au Muséum de Paris. *Bull. Mus. Nat. Hist. Nat.*, Paris, **8**: 184-187.

15) Lanchester, W. F., 1901. The Crustacea of the "Skeat" Expedition to the Malay Peninsula, together with a note on the genus *Actaeopsis*. Part 1, Brachyura, Stomatopoda and Macrura. *Proc. Zool. Soc. London*, **1901**: 534-574, pls. 33, 34.

16) Naiyanetr, P., 1994. On three new genera of Thai ricefield crabs allied to *Somanniathelphusa* Bott, 1968 (Crustacea: Decapoda: Brachyura: Parathelphusidae). *Raffles Bull. Zool.*, **42**: 695-700.

17) Ng, P. K. L., D. Guinot & P. J. F. Davie, 2008. Systema Brachyurorum: Part I. An annotated checklist of extant brachyuran crabs of the world. *Raffles Bull. Zool.*, Suppl. (17): 1-286.

18) Ng, P. K. L. & P. Naiyanetr, 1997. A revision of the genus *Siamthelphusa* Bott 1968 (Crustacea: Decapoda: Brachyura: Parathelphusidae), with description of five new species from Thailand. *J. Nat. Hist.*, **31**: 1751-1784.

19) Ng, P. K. L. & R. P. Lim, 1986. Description of a new genus and species of lowland freshwater crab from peninsular Malaysia (Crustacea, Decapoda, Brachyura, Parathelphusidae). *Indo-Malayan Zool.*, **3**: 97-103.

THE JOURNAL OF BIOLOGICAL CHEMISTRY VOL. 285, NO. 10, pp. 7739–7751, March 5, 2010

A CD36-related Transmembrane Protein Is Coordinated with an Intracellular Lipid-binding Protein in Selective Carotenoid Transport for Cocoon Coloration*[S]

Received for publication, October 9, 2009, and in revised form, January 5, 2010 Published, JBC Papers in Press, January 6, 2010, DOI 10.1074/jbc.M109.074435

Takashi Sakudoh[‡], Tetsuya Iizuka[§], Junko Narukawa[¶], Hideki Sezutsu[§], Isao Kobayashi[§], Seigo Kuwazaki[¶], Yutaka Banno[‖], Akitoshi Kitamura[**], Hiromu Sugiyama[‡‡], Naoko Takada[‡], Hirofumi Fujimoto[‡], Keiko Kadono-Okuda[¶], Kazuei Mita[¶], Toshiki Tamura[§], Kimiko Yamamoto[¶], and Kozo Tsuchida[‡1]

From the [‡]Division of Radiological Protection and Biology, National Institute of Infectious Diseases, Shinjuku, Tokyo 162-8640, the [§]Transgenic Silkworm Research Center and [¶]Insect Genome Research Unit, National Institute of Agrobiological Sciences, Tsukuba, Ibaraki 305-8634, the [‖]Genetic Resources Technology, Kyushu University, Fukuoka, Fukuoka 812-8581, the [**]Life Science Division, Fuji Chemical Industry Co., Ltd., Nakaniikawa, Toyama 930-0397, and the [‡‡]Department of Parasitology, National Institute of Infectious Diseases, Shinjuku, Tokyo 162-8640, Japan

The transport pathway of specific dietary carotenoids from the midgut lumen to the silk gland in the silkworm, *Bombyx mori*, is a model system for selective carotenoid transport because several genetic mutants with defects in parts of this pathway have been identified that manifest altered cocoon pigmentation. In the wild-type silkworm, which has both genes, *Yellow blood* (*Y*) and *Yellow cocoon* (*C*), lutein is transferred selectively from the hemolymph lipoprotein to the silk gland cells where it is accumulated into the cocoon. The *Y* gene encodes an intracellular carotenoid-binding protein (CBP) containing a lipid-binding domain known as the steroidogenic acute regulatory protein-related lipid transfer domain. Positional cloning and transgenic rescue experiments revealed that the *C* gene encodes *Cameo2*, a transmembrane protein gene belonging to the CD36 family genes, some of which, such as the mammalian *SR-BI* and the fruit fly *ninaD*, are reported as lipoprotein receptors or implicated in carotenoid transport for visual system. In *C* mutant larvae, Cameo2 expression was strongly repressed in the silk gland in a specific manner, resulting in colorless silk glands and white cocoons. The developmental profile of *Cameo2* expression, *CBP* expression, and lutein pigmentation in the silk gland of the yellow cocoon strain were correlated. We hypothesize that selective delivery of lutein to specific tissue requires the combination of two components: 1) CBP as a carotenoid transporter in cytosol and 2) Cameo2 as a transmembrane receptor on the surface of the cells.

All organisms exposed to light contain carotenoids, which are yellow to red C_{40} hydrophobic isoprenoid pigments. Carotenoids play pivotal roles in living organisms as precursors of vitamin A, antioxidants, and colorants (1). Their potential roles in medicine have recently been investigated. For example, macular accumulation of the carotenoids lutein and zeaxanthin is associated with a decreased risk of age-related macular degeneration (2), the leading cause of blindness in the developed world. Although plants, certain fungi, and bacteria synthesize carotenoids, animals appear to be incapable of synthesizing these molecules *de novo*. Therefore, animals must acquire carotenoids from dietary sources, and subsequently transport them to cells of target tissues.

The delivery of lipids, including carotenoids, to cells can be divided into three categories: 1) enzyme-mediated processes, such as the action of lipoprotein lipase on very low density lipoproteins, which converts a lipoprotein-bound lipid, triacylglycerol, into a water-soluble product, fatty acid, which diffuses into cells and leaves behind in the blood a lipoprotein product depleted in triacylglycerol (3); 2) receptor-mediated endocytosis, such as the uptake of low density lipoproteins by low density lipoprotein receptor, in which the entire lipoprotein particle is taken into the cell and metabolized (4); and 3) the delivery of specific lipids to specific tissues devoid of lipoprotein degradation, called selective lipid transport, such as the delivery of cholesterol ester from high density lipoprotein (HDL)[2] to the adrenal gland (5). The first two mechanisms have been extensively studied in vertebrates. However, the third mechanism, which clearly occurs in both vertebrates and invertebrates, is poorly understood.

In the domesticated silkworm, *Bombyx mori*, previous works have demonstrated the existence of tissue-specific delivery of

* This work was supported by the Kieikai Research Foundation (Japan), the Futaba Electronics Memorial Foundation (Japan), a grant-in-aid for scientific research from the Japan Society for the Promotion of Science, the Insect Technology Project of the Ministry of Agriculture, Forestry and Fisheries (Japan), and the National Bioresource Project (Silkworm) of the Ministry of Education, Culture, Sports, Science, and Technology (Japan).

[S] The on-line version of this article (available at http://www.jbc.org) contains supplemental "Experimental Procedures," Tables S1–S3, and Figs. S1–S5.

The nucleotide sequence(s) reported in this paper has been submitted to the GenBank™/EBI Data Bank with accession number(s) AB515345–AB515347.

[1] To whom correspondence should be addressed: 1-23-1 Toyama, Shinjuku, Tokyo 162-8640, Japan. Tel.: 81-3-5285-1111 (ext. 2421); Fax: 81-3-5285-1194; E-mail: kozo@nih.go.jp.

[2] The abbreviations used are: HDL, high density lipoprotein; *C*, *Yellow cocoon*; Cameo, *C* locus-associated membrane protein homologous to a mammalian HDL receptor; CBP, carotenoid-binding protein; SR-BI, scavenger receptor class B type I; RT, reverse transcriptase; SNP, single nucleotide polymorphism; START, steroidogenic acute regulatory protein-related lipid transfer; UAS, upstream activating sequence; IV0, day 0 of the fourth instar; V0, day 0 of the fifth instar; W0, day 0 of the wandering stage; *Y*, *Yellow blood*; HPLC, high-performance liquid chromatography; EGFP, enhanced green fluorescent protein.

Cameo2 Is Coordinated with CBP in Carotenoid Transport

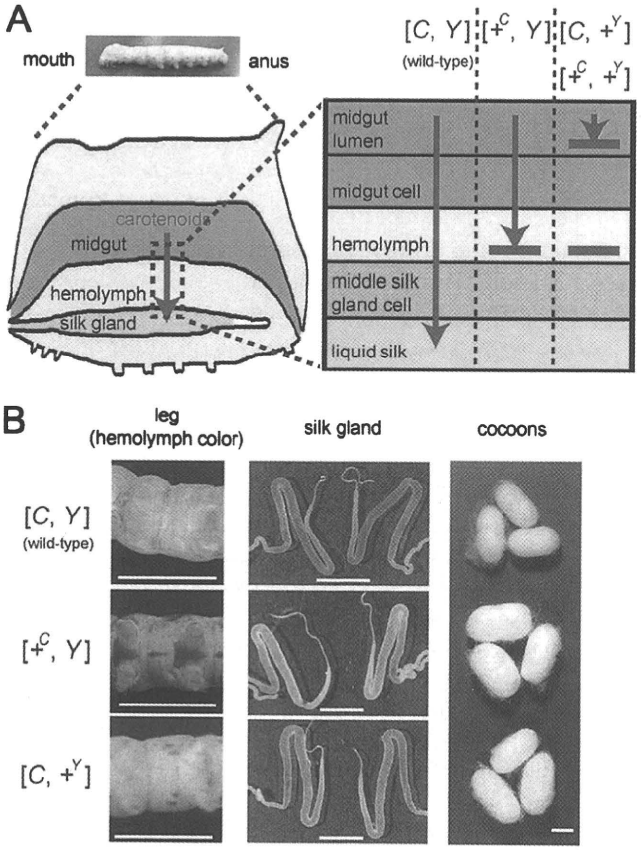

FIGURE 1. **Transport of lutein by the *Yellow cocoon* (*C*) gene and the *Yellow blood* (*Y*) gene.** *A*, schematic representation of the functions of the *C* and *Y* genes in the carotenoid transport system of the silkworm. $+^C$ and $+^Y$ represent a recessive allele of the *C* and *Y* genes, respectively. *B*, color phenotype of the hemolymph, silk gland, and cocoons. The hemolymph color is visible on the abdominal legs where the skin is relatively transparent. The silk glands are paired organs. The c10, c05, and FL501 ($+^Y$) strains were used as the genotypes of [*C*, *Y*], [$+^C$, *Y*], and [*C*, $+^Y$], respectively. The silkworm with the genotype of [$+^C$, $+^Y$] exhibits colorless hemolymph and produces white cocoons, similar to [*C*, $+^Y$]. Legs were at day 3 of the fifth larval instar (V3). Silk glands were at day 0 of the wandering stage (W0). The lutein content of the middle silk gland of [*C*, *Y*] was about 30-fold higher than that of [$+^C$, *Y*] (data not shown). The *black* color of the larval skin of the c05 strain was due to the larval marker gene, p^S. *Scale bar*, 1 cm.

specific carotenoids (6–9). The wild-type silkworm feeds on carotenoid-rich mulberry leaves in the larval stage. Carotenoids are then absorbed into the midgut epithelium, transferred to the hemolymph lipoprotein, lipophorin, and accumulated in the middle silk gland, resulting in yellow hemolymph and the formation of a yellow cocoon (Fig. 1, *A* and *B*). Lipophorin facilitates lipid transport in insects in a selective manner (10). Over the 4000 year history of sericulture, several mutants have been noted that produce white cocoons due to defect in carotenoid transport (11). Among these are mutants in the selective transport of carotenoids from lipophorin to the middle silk gland. Molecular cloning of the genes responsible for these mutants therefore provides tools to determine the molecular mechanism of selective carotenoid transport.

The *Yellow blood* (*Y*) gene on chromosome 2 of *B. mori* controls transport of carotenoids from the midgut lumen to the midgut epithelium and from the lipophorin to the middle silk gland cells (Fig. 1*A*) (7–9). We have reported previously that the *Y* gene encodes an intracellular carotenoid-binding protein (CBP) (12), which was identified based on a combination of expression analysis (12, 13), restriction fragment length mapping (14), genomic sequence analysis (15, 16), and transgenic rescue of phenotype (16). CBP is a 33-kDa protein containing a lipid-binding domain known as the steroidogenic acute regulatory protein-related lipid transfer (START) domain (17). CBP is expressed in the midgut, the middle silk gland, testis, and ovary in the dominant *Y* allele strain ("*X* allele strain" represents the strain harboring the homozygous *X* allele), producing yellow cocoons. In *Y* mutants homozygous for the recessive $+^Y$ allele, genomic deletion of the *CBP* gene leads to complete absence of the CBP protein. The midgut epithelium, therefore, poorly absorbs carotenoids, resulting in colorless hemolymph, colorless middle silk gland, and white cocoons (Fig. 1*B*).

The *Yellow cocoon* (*C*) gene on chromosome 12 controls transport of carotenoids, mainly lutein, from lipophorin to the middle silk gland cells (Fig. 1*A*) (11, 18). The middle silk glands of the *C* mutants, homozygous for the recessive $+^C$ allele, have a defect in the cellular uptake of lutein and are, therefore, colorless even in the presence of yellow hemolymph mediated by the dominant *Y* allele of the *Y* gene, resulting in white cocoons (Fig. 1*B*). Selective transport of lutein from lipophorin to middle silk gland cells by the dominant *C* allele requires the *Y* allele (19, 20). Thus, molecular cloning of the *C* gene was expected to offer a novel molecular component that facilitates selective transport of lutein in coordination with CBP in middle silk gland cells.

In the present study, the *C* gene was cloned using a positional cloning method, resulting in identification of Cameo2 (Cameo locus associated membrane protein homologous to a mammalian HDL receptor-2). Cameo2 belongs to the CD36 family, including scavenger receptor class B type I (SR-BI), a transmembrane receptor of mammalian HDL (5). A molecular pathway for selective lutein transport in the body of the silkworm by a combination of Cameo2 and CBP is proposed.

EXPERIMENTAL PROCEDURES

Silkworm Strains—The c04, c05, c10, c11, c43 (*Pk*), e09, FL501 ($Y/+^Y$), and FL501 ($+^Y/+^Y$) strains have been preserved at the silkworm stock center of Kyushu University, Fukuoka, Japan. The number 925 and w1-pnd strains have been preserved in the National Institute of Agrobiological Sciences, Ibaraki, Japan. The N4 strain has been preserved at the National Institute of Infectious Diseases, Tokyo, Japan. The Kinshu X Showa F1 hybrids were a generous gift from Dr. Toru Shimada (University of Tokyo, Tokyo, Japan). The larvae were reared on mulberry leaves or an artificial diet made from mulberry leaves (Nihon Nosan Kogyo Co., Yokohama, Japan). Data regarding the origin, genotype, and phenotype of these strains are summarized in supplemental Table S1. The first days corresponding to the developmental stages of the third to fourth larval ecdysis, the fourth to fifth larval ecdysis, and wandering, a characteristic behavior with enhanced locomotory activity just before spinning cocoons, were designated as IV0, V0, and W0, respectively.

Crossing and Genomic Extraction for Mapping of the C Gene—Two silkworm strains, c11 (*C*/*C*, *Y*/*Y*, yellow cocoon with yel-

low hemolymph) and number 925 ($+^{C}/+^{C}$, *Y/Y*, white cocoon with yellow hemolymph) were used. Single-pair crosses between number 925 and c11 produced F1 offspring. As female recombination is uncommon in *B. mori* (21), BF1 progeny from the single-pair cross between female number 925 and males of F1 (number 925 X c11) were used for recombination mapping. The number of single-pair matings for BF1 progeny was 18. Each of the total of 1775 BF1 individuals was named, phenotypically recorded, and subjected to genomic DNA extraction using DNAzol Reagent (Invitrogen). None of the BF1 individuals analyzed showed colorless hemolymph.

Mapping Using Single Nucleotide Polymorphism (SNP) Markers—For mapping using the BF1 progeny, PCR primer sets were generated at each position on chromosome 12, and primer sets with that the PCR products showed polymorphism between parents were used for SNP markers. The PCR primers used for SNP analysis are listed in supplemental Table S2. The PCR products treated with ExoSAP-It (U. S. Biochemical Corp.) were subjected to direct sequencing.

RNA Extraction—Total RNA was isolated from tissues washed in insect saline (20 mM sodium phosphate buffer, 150 mM sodium chloride, pH 6.7) with TRIzol reagent (Invitrogen). Before addition to TRIzol reagent, the silk gland and midgut were frozen in liquid nitrogen and broken into fine pieces. The other tissues were syringe-homogenized in TRIzol reagent.

Comparison of the Cameo1 and Cameo2 cDNA Sequences between the C and $+^{C}$ Allele Strains—*Cameo1* and *Cameo2* were amplified from the middle silk gland of each strain via reverse transcription (RT)-PCR and directly sequenced. The PCR primers used for each gene and strain are listed in supplemental Table S3.

Data Base Search for Cameo1 and Cameo2 Homologs in the Silkworm—The silkworm genome contained 13 annotated genes homologous to *Cameo1* and *Cameo2*, which were retrieved from the KAIKObase system through a keyword search using "CD36" as the query. The TBLASTN program was used to search for all genes homologous to *Cameo1* and *Cameo2* in the silkworm genome sequence (22) and EST data base (23) with a cutoff *E* value of 5×10^{-3} and the results did not include any others besides these 13 genes. One of these homologous genes, *SNMP1*, has been cloned (24), and recently 10 of them were reported and named by independent data base searches (25, 26). We use in this paper the same names for the total 11 genes and term the other two genes, BGIBMGA13436 and BGIBMGA13438 in the China gene model ("BGIBMGA" is a prefix for gene name), SCRB14 and SCRB15, respectively.

Phylogenetic Analysis of the Protein Sequences Homologous to Cameo1 and Cameo2—Alignment of the hypothetical protein sequences was performed using Clustal W2 (27). A phylogenetic tree was then constructed with the neighbor-joining method using Clustal X2 (27).

Northern Blotting—For *Cameo2*, a ^{32}P-labeled riboprobe was synthesized from the N-0394 EST clone. The insert of N-0394 contained the 3′ part (1016 bp) of the open reading frame and the 5′ part (1209 bp) of the 3′-untranslated region of *Cameo2*. No silkworm repetitive sequence was found in the insert. Total RNA was electrophoresed on 1% agarose gels containing formaldehyde and transferred onto Hybond N^{+} membrane (GE Healthcare UK). Hybridization was performed with Ultrahyb (Ambion, Austin, TX).

RT-PCR Analysis of Tissue Distribution of Cameo1, Cameo2, and rpL3—Primer1-1 (5′-CTGAAAGTGGAGCAGTTGGGTCCTTACG-3′) and Primer1-4 (5′-CGGACACCTTGACGACCCTGGGCTGGTG-3′) for *Cameo1*, Primer2-3 (5′-GGACCAGGTCACCGGCATGAACCCGGATC-3′) and Primer2-2 (5′-CGTCCTCAGCTCCGAAATGATTTTTGGATC-3′) for *Cameo2*, and Primer-rpL3-real-cDNA1 (5′-TTCCCGAAAGACGACCCTAG-3′) and Primer-rpL3-real-cDNA2 (5′-CTCAATGTATCCAACAACACCGAC-3′) for *rpL3* were used.

Analysis of Carotenoid Composition of the Middle Silk Gland—Samples of the middle silk gland cut into small pieces less than 1 mm length (~200 mg) were transferred into a glass centrifuge tube with 5 ml of distilled water and 2 g of glass beads (1 mm diameter) as agitating aid were added. After heating at 90 °C for 15 min, eluate was collected. 5 ml of 80% ethanol with butylhydroxytoluene as an antioxidizing agent at a concentration of 10 μg/ml was added to the residue, followed by heating at 90 °C for 10 min with vortexing at intervals. The eluate was then collected. Extraction with 80% ethanol was repeated three times. 3 ml of 100% ethanol with butylhydroxytoluene was added to the residue, followed by heating at 90 °C for 10 min with vortexing at intervals. The eluate was then collected. Extraction with ethanol was repeated until the residue became colorless. All of the collected extracts were pooled, and ethanol was evaporated. 1 g of sodium sulfate decahydrate was then added followed by extraction three times with 5 ml of petroleum ether. 9 ml of acetone was added to the aqueous layer, then extracted with 5 ml of petroleum ether three times. The organic phase was dried over anhydrous sodium sulfate and evaporated. The residue was resolved in acetone and used for carotenoid analysis by high performance liquid chromatography (HPLC). A reverse-phase column (YMC carotenoid 5 μm (4.6 × 250 mm); Waters Co., Milford, MA) was used under the following conditions: temperature, 25 °C; flow rate, 1 ml/min; mobile phase, A, methanol; B, *t*-butylmethylether; C, 1% (v/v) aqueous phosphoric acid; a 15-min linear gradient from 81% A, 15% B, 4% C to 66% A, 30% B, 4% C; an 8-min linear gradient to 16% A, 80% B, 4% C, a 4-min hold at 16% A, 80% B, 4% C, then back to 81% A, 15% B, 4% C, and an 8-min hold at 81% A, 15% B, 4% C.

Quantification of Transcripts by Real Time PCR—Single-stranded cDNAs from various tissue samples were synthesized from total RNAs with Superscript III reverse transcriptase (Invitrogen) with oligo(dT) primer, and treated with RNase H (Takara, Kyoto, Japan). Quantification of transcripts was carried out by real time PCR using these cDNAs as templates with LightCycler FastStartDNA MasterPLUS SYBR Green I (Roche) and LightCycler DX400 (Roche). The primer pairs used for detection of *Cameo1*, *Cameo2*, *CBP*, and *rpL3* were Primer1-1 and Primer1-6 (5′-CGCCACAGTCGCTATTATAGGGTTGATGC-3′); Primer2-19 (5′-AGTGTTAGAGGAGGTGCACCAGCTC-3′) and Primer2-16 (5′-CAGTCCGTTTTGAACCCCACTCTCC-3′); PrimerCBP-1 (5′-ATGGCCGACTCTACGTCGAAAAGCG-3′) and PrimerCBP-18 (5′-GCCTTCAACTTTCCTTGACTCCACGACG-3′); and Primer-rpL3-real-cDNA1 and Primer-rpL3-real-cDNA2, respectively. For *Cameo1*, *Cameo2*, and *rpL3*, absence of mutation in the anneal-

ing sites of these primers among the analyzed strains was confirmed (supplemental Fig. S2). Serial dilutions of plasmids containing the cDNA sequences were used as standards. Transcript levels of *Cameo1*, *Cameo2*, and *CBP* were normalized with the level of the *rpL3* transcript in the same samples, as described previously (28).

Analysis of F1 SNPs of Cameo1 and Cameo2—The cDNA sequences of *Cameo1* and *Cameo2* of each parental strain were aligned (supplemental Fig. S2). Then primer pairs, Primer1-3 (5′-GAGGGCGTTCGGTACGCGGCCAACGACTC-3′) and Primer1-2 (5′-CTGGATCTTGCTGGGGTAGTACGGGTC-3′) for *Cameo1*, Primer1-25 (5′-TATCAACAACGTGTTGC-CGGACC-3′) and Primer1-16 (5′-GTGAGGGTGTAGAGC-GCGTATG-3′) for *Cameo1*, Primer2-19 and Primer2-16 for *Cameo2*, and Primer2-21 (5′-TCCTTACCGTTACCAGGAG-CATAG-3′) and Primer2-20 (5′-GCGGTTATAACGTCAAT-GGTTGTG-3′) for *Cameo2* were designed according to the conserved nucleotide sequence for PCR amplification of the cDNA and genomic DNA of the parental and F1 strains, and the PCR products by these primer pairs were directly sequenced with Primer1-2, Primer1-25, Primer2-18 (5′-TTG-GAGCATTCGCCGTCG-3′), and Primer2-21, respectively.

Western Blotting—A rabbit polyclonal antibody against Cameo2 was raised against the synthetic peptide (C-)NGLKY-NKYEVNERS (amino acids 295–308, corresponding to the putative extracellular domain (Fig. 3*B*)) coupled to keyhole limpet hemocyanin and affinity purified by Operon Biotechnologies (Tokyo, Japan). For Western blotting analysis of the membrane fraction, 100 pieces of the silk gland of each strain on the day 0 of the wandering stage (W0) was homogenized in ice-cold insect saline containing a protease inhibitor mixture (Protease Inhibitor Mixture Set III, EDTA-free, Calbiochem, San Diego, CA) using a Polytron homogenizer. The homogenate was centrifuged at 800 × *g* for 10 min, and the supernatant was filtered through cheesecloth and centrifuged at 1,000 × *g* for 10 min. The membranes were then pelleted by centrifugation at 100,000 × *g* for 1 h and resuspended in 20 mM Tris-HCl, 150 mM NaCl, 2 mM $CaCl_2$, 0.1 mM phenylmethylsulfonyl fluoride, pH 7.4, at a concentration of 10 mg of protein/ml. Then, the same volume of 80 mM *n*-octylglucoside was added for solubilization. After mixing for 1 h, insoluble material was removed by centrifugation at 100,000 × *g* for 1 h. The concentration of *n*-octylglucoside in soluble extract was adjusted to 5 mM by addition of 7 volumes of 20 mM Tris-HCl buffer, and centrifuged at 100,000 × *g*, 1 h to collect precipitate. The pellet was resuspended again in 20 mM Tris-HCl, 150 mM NaCl. The protein concentration was determined with the Bradford method (Protein Assay solution; Bio-Rad). Then, 25 μg of protein was separated by SDS-PAGE, transferred to polyvinylidene difluoride membrane, and probed with the anti-Cameo2 antibody and a sheep anti-rabbit IgG-conjugated alkaline phosphatase (Jackson ImmunoResearch Laboratory, West Grove, PA). The signals were detected by AP-conjugate Substrate Kit (Bio-Rad).

Immunohistchemistry—Cross-sections of the middle silk gland from the region of "MSG-3" in Fig. 5*C* were deparaffinized in xylene, rehydrated through graded ethanol solutions, and quenched with a 30-min immersion in 0.3% hydrogen peroxide in methanol. Sections were blocked for 30 min in normal goat serum in phosphate-buffered saline, and incubated with the Cameo2 antibody (at 1:1000 dilution) used for the Western blotting experiment overnight at 4 °C. Sections were rinsed in phosphate-buffered saline, and incubated for 30 min with a biotinylated goat anti-rabbit IgG (at 1:200 dilution). The slides were developed using the ABC Vectastain Elite kit (Vector Labs, Burlingame, CA) following the manufacturer's instructions. The slides were counterstained in Mayer hematoxylin.

Silkworm Transgenesis—We first attempted to produce the nondiapausing strain with the phenotype of yellow hemolymph and white cocoons. The number 925 strain of the genotype [Y, $+^C$] was crossed with the w1-pnd strain, a nondiapausing strain with the genotype [$+^Y$, $+^C$] used for transgenesis of *B. mori* (29). By sib mating of the progeny, a nondiapausing strain with the phenotype of yellow hemolymph and white cocoons, termed w1-pnd-925, was established.

For transgenic expression of Cameo2 in the w1-pnd-925 strain by the binary GAL4/upstream activating sequence (*UAS*) system (30), *Cameo2* was amplified by RT-PCR from the middle silk gland of the N4 strain with Primer2-13 (5′-ATGCTCTAG-ATTCCTTGTGATAATCGCGGC-3′) and Primer2-10 (5′-ATGCTCTAGACATACGGACTCATTCCAATG-3′), both of which have an XbaI site. The PCR product was subcloned into the pGEM T-vector, and the subcloned product was digested with XbaI. The fragment was ligated into the vector *pBacMCS-[UAS-3xP3-EGFP]* (16) previously digested with BlnI. The resulting effector construct *pBacMCS[UAS-Cameo2-3xP3-EGFP]* was confirmed by DNA sequencing. For the effector strains, the effector construct and the helper plasmid, pHA3PIG (29), were injected into preblastoderm embryos of the w1-pnd-925 strain at a concentration of 0.2 mg/ml. After sib selection based on the presence of EGFP fluorescence in the eye by the *3xP3-EGFP* gene, G1 male moths of a UAS-Cameo2 (UAS) line with the phenotype of yellow hemolymph and white cocoons were crossed with females of the Ser1-GAL4 (GAL4) line with the phenotype of colorless hemolymph and white cocoons, which drives target gene expression in the middle silk gland and has a marker fluorescence in the eye by the *3xP3-DsRed* gene (31). Because the transgene was supposed to be homozygous in the GAL4 line, the progeny of the cross between the UAS line and GAL4 line showed two different marker phenotypes of eye color: both DsRed- and EGFP-positive, GAL4/UAS line (Ser1-GAL4(+), UAS-Cameo2(+)); and only DsRed-positive, GAL4 line (Ser1-GAL4(+), UAS-Cameo2(−)). Data from the individuals exhibiting colorless hemolymph in the larval stage, which had colorless silk glands and produced white cocoons, were not presented in Fig. 7, *B–E*. Experimental procedures for determination of the *Cameo1* and *Cameo2* cDNA sequence and Southern blotting are described under supplemental data.

RESULTS

Mapping of the C Locus—To identify a candidate physical region for the *C* locus, we performed genetic linkage analysis using SNP markers (32, 33). First, the *C* locus was roughly mapped with 75 BF1 individuals, and the *C*-linked region was narrowed to the 1.94 Mb range on chromosome 12 between two SNP markers, 12-055 and 12-056 (Fig. 2*A*). Then, novel

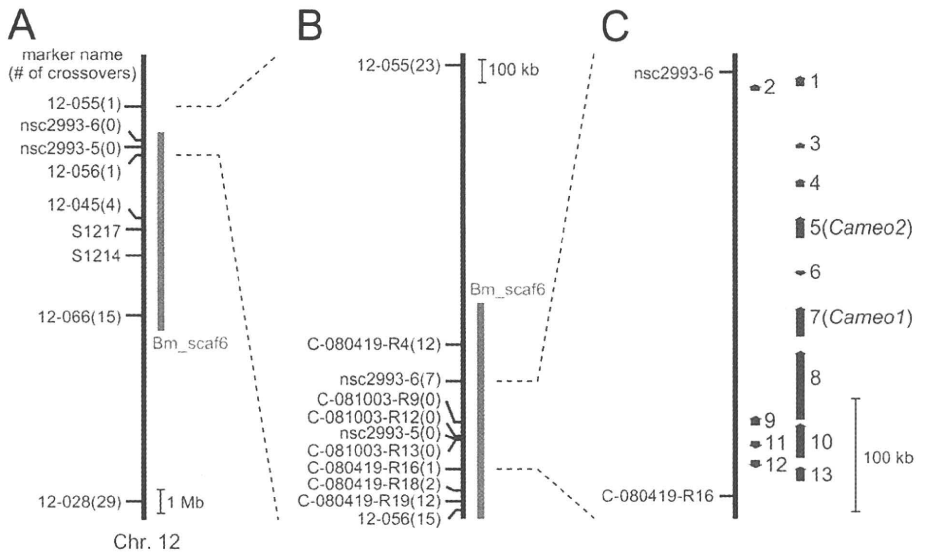

FIGURE 2. **Mapping of the *C* gene on the chromosome 12.** *A*, rough mapping with 75 individuals. *Small horizontal lines* on the *vertical bars* of chromosome 12 denote the positions of crossover events with the name of the SNP maker and the number of recombinants. Recently, Li and colleagues (63) independently showed that the *C* locus was closer to SSR marker S1217 than S1214, consistent with our results. *B*, finer mapping with 1700 individuals. *C*, physical map of chromosome 12 near the *C* locus with the predicted gene. *Vertical arrows* indicate the orientation and relative size of the 13 putative genes predicted by the China gene model (22). *1*, BGIBMGA010481 (SMAD homolog); *2*, BGIBMGA010480 (unknown); *3*, BGIBMGA010479 (unknown); *4*, BGIBMGA010478 (similar to the CG7231 gene of *D. melanogaster*, whose molecular function is unknown); *5*, BGIBMGA010477 (*Cameo2*); *6*, BGIBMGA010502 (unknown); *7*, BGIBMGA010476 (*Cameo1*); *8*, BGIBMGA010475 (dynein heavy chain homolog); *9*, BGIBMGA010474 (dynein heavy chain homolog); *10*, BGIBMGA010473 (dynein heavy chain homolog); *11*, BGIBMGA010503 (homolog of SprT-like metalloproteases with zinc finger domain); *12*, BGIBMGA010504 (tetraspanin homolog); *13*, BGIBMGA010472 (similar to muscle-specific protein 300, involved in cytoskeleton organization).

primer sets were designed in the narrowed range, and finer mapping was performed with 1700 BF1 individuals. As a result, the *C*-linked region was further narrowed to the 375-kb range between two SNP markers, nsc2993-6 and C-080419-R16, which was on one scaffold, Bm_scaf6 (Fig. 2*B*).

Candidates for the C Gene—Thirteen genes were predicted within the narrowed region by the China gene model at KAIKObase (22) (Fig. 2*C*). Among them, two genes were found to encode proteins homologous to SR-BI, a mammalian transmembrane cell surface receptor for HDL (5, 34–36). SR-BI mediates cellular uptake of cholesteryl ester from HDL in a selective manner. SR-BI was proposed to form a hydrophobic channel along which cholesteryl esters migrate (37). Furthermore, mutants of the *ninaD* gene, a homolog of SR-BI in the fruit fly *Drosophila melanogaster*, was reported to affect carotenoid uptake in gut for visual chromophore synthesis (38–40), and SR-BI was also implicated in cellular carotenoid absorption (41–44). Therefore, we considered these two genes to be strong candidates for the *C* gene, and designated the gene nearer the SNP marker C-080419-R16 *Cameo1* and the other *Cameo2*.

Characterization of the Cameo1 and Cameo2 Sequences—We determined each cDNA sequence containing the full-length of the open reading frame of *Cameo1* and *Cameo2* from a *C* allele strain. *Cameo1* and *Cameo2* span a region of 120 kb in the Bm_scaf6, and are composed of 11 and 10 exons, respectively (Fig. 3*A*). The deduced amino acid sequence indicated that Cameo1 and Cameo2 are a 56.2-kDa protein of 495 amino acids and a 56.0-kDa protein of 494 amino acids, respectively (Fig. 3*B*). The degree of identity between Cameo1 and Cameo2 is 28%. Cameo1 and Cameo2 share 32 and 26% amino acid identity, respectively, with the human SR-BI and 32 and 31% identity, respectively, with the fruit fly NinaD. TMHMM version 2.0 (45), software for prediction of transmembrane helices, predicted that both gene products are comprised of a large extracellular loop, anchored to the plasma membrane on each side by transmembrane domains adjacent to short cytoplasmic N-terminal and C-terminal domains (Fig. 3*B*). SignalP 3.0-HMM (46), a program for prediction of signal peptide, predicted that the N termini of Cameo1 and Cameo2 are signal peptides with a probability of 29 and 95%, respectively. The cleavage site with maximum probability was near the C terminus of the N-terminal putative transmembrane domain in Cameo1 and Cameo2, respectively (Fig. 3*B*, *arrow*). Therefore, we tentatively propose that Cameo1 and Cameo2 are single- or double-pass transmembrane proteins (Fig. 3*C*). It could be noted that the existence of the N-terminal transmembrane helix in SR-BI homologs, CD36 family genes, has been a matter of debate (5, 47), and some of them were similarly predicted to have a single- or double-pass transmembrane structure at various ratios (Fig. 3*C*).

There are 13 other genes homologous to *Cameo1* and *Cameo2* in the silkworm genome data base (22). These genes were distributed or tandemly positioned in several chromosomes (Fig. 3*D*). No homologous genes other than *Cameo1* and *Cameo2* were found on chromosome 12, where the *C* locus lies. The phylogenetic tree of these silkworm genes was generated with the CD36 family genes from insects and mammals (Fig. 3*E*). As indicated in a previous study in Dipterans (48), the insect genes could be largely divided into three groups, and *Cameo1* and *Cameo2* fall into the Group 2. Group 2 contains functionally characterized genes of *D. melanogaster*. *Santa maria* is implicated in cellular uptake of carotenoids in extraretinal neural cells in heads (40), *crq* is required for efficient phagocytosis of apoptotic cells (49), and *pes* was identified as a host factor required for the uptake of mycobacteria (50). The orthologous relationships of the Group 2 genes were not clear. SNMP in Group 3 is required for chemoreception of (*Z*)-11-octadecenyl acetate in olfactory neurons of *D. melanogaster* (24, 51, 52). The mammalian homologs formed a distinct group. CD36 is implicated in cellular uptake of long-chain fatty acids (53).

Comparison of the Nucleotide Sequences of Cameo1 and Cameo2 between the C and $+^C$ Allele Strains—Southern blotting analysis suggested that the silkworm has a single copy of

Cameo2 Is Coordinated with CBP in Carotenoid Transport

the *Cameo1* and *Cameo2* genes irrespective of the genotype of the *C* gene (supplemental Fig. S1). Then, to examine the relationship between the *C* gene with *Cameo1* and *Cameo2*, we compared the mRNA sequences of *Cameo1* and *Cameo2* among three *C* allele strains and four $+^{C}$ allele strains (supplemental Fig. S2). The mRNA sequences of *Cameo1* and *Cameo2* were well conserved and absent of indels and premature stop codons, whereas one nonsynonymous mutation in Cameo1

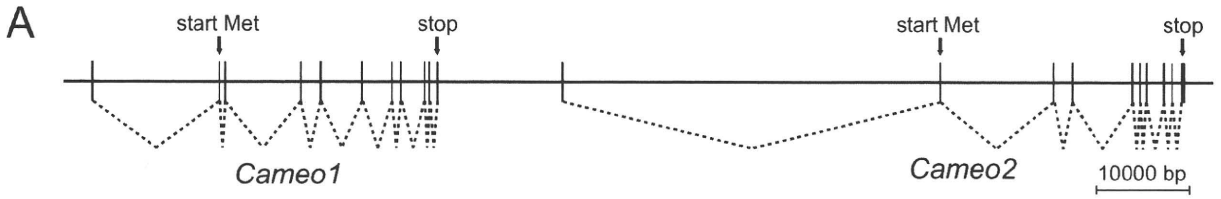

B

```
Cameo1    1: MKMVSSGV-KSG-LFMGFGSAL-VLIGAIVV-VYWPSLFMAQLQRMMILSPISISFGIWQ 56
Cameo2    1: --MRG-GLLRWRSLWICGG-ALLALS-AFVAALTWGAIFDSAFGSQLALTPDSRSFMRWL 55

Cameo1   57: ETPIPMYLECYMFNITNADKILAKEDVILKVEQLGPYVFRESHSKVNLTWN-DNSTIIFY 115
Cameo2   56: EPDVPIFFDIYMFNWTNPERFPEEKPN-F--EEIGPYRYQEHRRHVNISWHPENGTIGYR 112

Cameo1  116: NQRFWHFDQNLSKGSLSDEIIS-INPIIATVAYIVRHQPRVVKVSVDVFLRMFHDDLF-L 173
Cameo2  113: TLRSWVWDESSV-GSQ-DDLITTIDVITASAIYQARFSGFIEQKIVSLTLTSSQHTKVSV 170

Cameo1  174: KANVSSWLFEGIEDPVLEMAQKFPDLPLNI-PY-DKFGWFYERNGSREFDGSFI-MNT-G 229
Cameo2  171: TARASEFLFEGMEDPLLNLAKLMPASVRGGAPAIDRFGWFFSRNNTDT-DG-YMEV-DSG 227

Cameo1  230: AADFSRL-GNIEL-WKYSPRTVFRDH-CGDVKGSTGELWAPELGQPELFV-FASDICTYL 285
Cameo2  228: TRDG--LPGQI-LRWNYQDHIPEYDGECSKLSGSAGEYIPRNLTEDSKLTMYVPDLCRTV 284

Cameo1  286: TLHKKEDVLIENIEGVRYAANDSLFDNGHKYPAMACYCDEVRDRDCVPPGALNVSLCRLG 345
Cameo2  285: NMEFVESGVQNGLKYNKYEVNERSFDNSSTSPENTCFCKG-----ECAWGGVMNVSACRFG 340

Cameo1  346: APAFVSQPHFLDADPYYPSKIQGLDPQEE-HRFSLALEM-FTGMPLAVSAQLQINLLIRD 403
Cameo2  341: SPAFITLPHFLHGDPALLDQVTGMNPDPDKHSEYFAMEPKL-GVPIDVAGRFQFNVYVEP 399

Cameo1  404: VWG-ISINNVLPDPDIM-VPMFWFRQELQVTPEYAHMARVALA-LRYYTPY--ALYTLTV 458
Cameo2  400: -SDHITLYENMPR---MLFPVFWVEQKAKIDPKIISELRTVRGILD-WGETFCACFAVV- 453

Cameo1  459: IGVVLILVGVVVLIRRLLNSSDTTPLIEESA-SQ-ENQQ----- 495
Cameo2  454: IAL-L-VTAITCCTKRTEYTRPHDIL-KPYEKPKDEAEMKLNPI 494
```

C

	double-pass	single-pass
		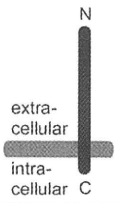
Cameo1	70 %	29 %
Cameo2	5 %	95 %
SR-BI (human)	32 %	68 %
SR-BI (mouse)	35 %	65 %
CD36 (human)	93 %	7 %
NinaD	84 %	15 %
Santa maria	97 %	3 %

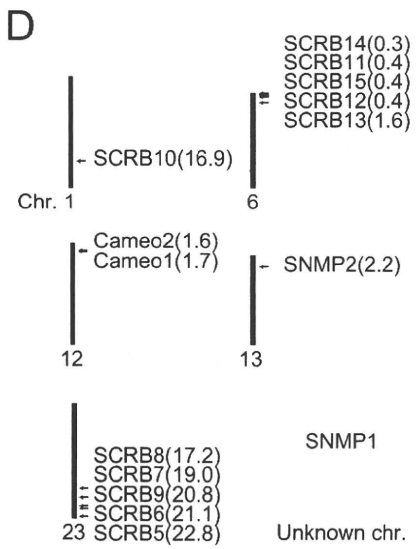

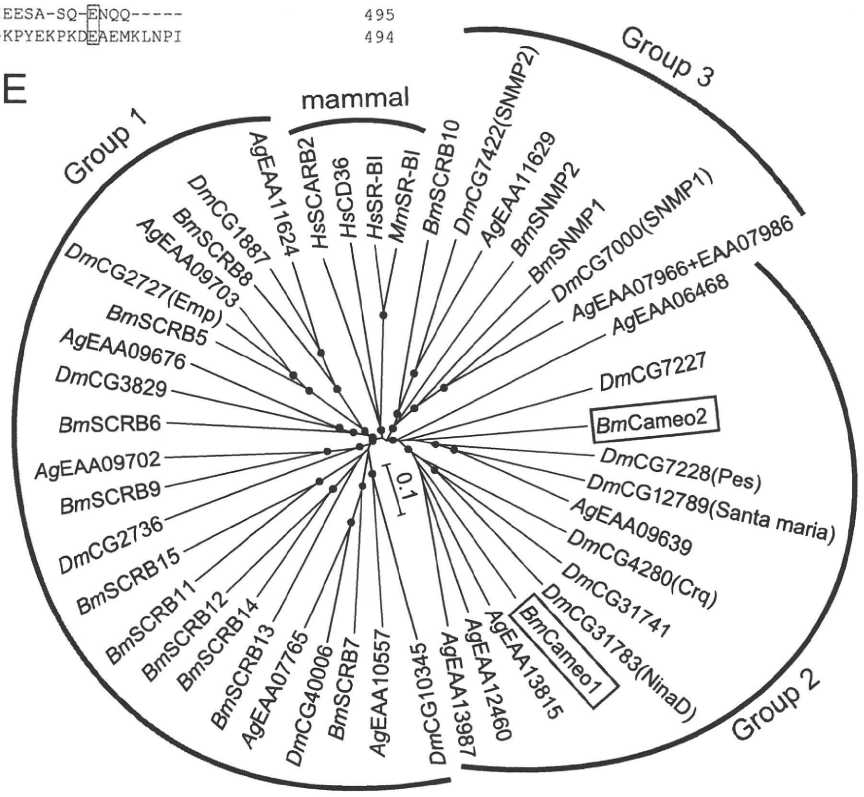

(from lysine to asparagine at amino acid position 315; K315N) was found in all of the $+^C$ allele strains and three nonsynonymous mutations in Cameo2 (V124A, V293I, and S431L) were found in part of the *C* allele strains.

Expression of Cameo2 Was Significantly Reduced in the Middle Silk Gland of the $+^C$ Allele Strain—We next examined *Cameo1* and *Cameo2* expression in the middle silk gland with multiple *C* and $+^C$ allele strains by Northern blotting analysis. With probes for *Cameo1*, no specific signal has yet been detected (data not shown). Using a ^{32}P-labeled riboprobe for *Cameo2*, one significant signal of relatively large size (>6.5 kb) and another weaker signal of smaller size (≈3.5 kb) were obtained in *C* allele strains on day 0 of the wandering stage (W0), when the larvae exhibit a characteristic behavior with enhanced locomotory activity just before spinning cocoons in the fifth instar (Fig. 4*A*). The signals were significantly reduced in each of the $+^C$ allele strains. The *Cameo2* signal in the FL501 [$+^Y$, *C*] strain, in which the hemolymph and silk gland were colorless due to the homozygous $+^Y$ allele, was not reduced to the level of the $+^C$ allele strains, suggesting that *Cameo2* expression was controlled by the *C* locus rather than lutein accumulation in the middle silk gland.

To examine protein expression of Cameo2, we prepared a rabbit polyclonal antibody for a 14-residue peptide in the predicted extracellular region that shows a low sequence similarity to Cameo1 (Fig. 3*B*). This antibody recognized a protein of ≈68 kDa in the membrane fraction of the silk gland of the *C* allele strain, but not in the $+^C$ allele strain (Fig. 4*B*), consistent with Northern blotting analysis (Fig. 4*A*). The difference between the observed and predicted molecular masses of Cameo2 (56.0 kDa in the double-pass transmembrane model and 52.7 kDa in the single-pass transmembrane model) may be due to post-translational glycosylation at asparagine residues (Fig. 3*B*). Differences between the observed and predicted molecular masses have been observed in other CD36 family genes (5). Immunohistochemistry demonstrated that the immunoreactivity for the antibody was found on the apical surface of the middle silk gland (Fig. 4*C*), which would have direct contact with the hemolymph.

Developmental and Regional Expression Profiles of Cameo1, Cameo2, and CBP in the Middle Silk Gland—Lutein pigmentation in the middle silk gland of the *C* allele strain is known to be under developmental regulation, whereas the $+^C$ allele strain remains colorless (8, 54) (Fig. 5*A*). To examine the relationship with lutein accumulation, the developmental profiles of *Cameo1* and *Cameo2* mRNA expression in the middle silk glands of both the *C* and $+^C$ allele strains were analyzed by quantitative RT-PCR from day 0 to 3 of the fourth instar (IV0-IV3) and from day 0 to 7 or 8 of the fifth instar (V0–V7 or -V8) (Fig. 5*B*). In the *C* allele strain, the expression of *Cameo1* and *Cameo2* reached a small peak on IV2, declined to a low level around the time of molting between the fourth and fifth instars, and then increased and peaked again in the middle-late fifth instar. The degree of increase in *Cameo2* expression during the fifth instar was remarkably high, showing an approximate 500-fold difference between V0 and V5. This significant increase in *Cameo2* expression during the fifth instar was consistent with the increment of the pigmentation from V3 or V4 (Fig. 5*A*). On V7, the day before pupation, *Cameo2* expression decreased markedly from V6, whereas *Cameo1* expression remained elevated. This drop in *Cameo2* expression was consistent with the loss of requirement of pigmentation for cocoon coloration because the larvae had stopped spinning and the silk gland was undergoing degradation. In the $+^C$ allele strain, the developmental profile of *Cameo1* expression was similar to that of the *C* allele strain, suggesting that the *C* locus does not largely affect *Cameo1* expression in the middle silk gland. In contrast, *Cameo2* expression was significantly lower than that observed in the *C* allele strain on all days, with a small peak on V3–V5. The lower level of *Cameo2* expression was consistent with the Northern and Western blotting analyses (Fig. 4) and the reduced degree of pigmentation in the fifth instar (Fig. 5*A*).

We separated the middle silk gland of the *C* allele strain at W0 into five sections (Fig. 5*C*), and examined *Cameo1* and *Cameo2* expression in each section by quantitative RT-PCR (Fig. 5*D*). *Cameo2* expression was significantly higher in the middle three sections than in the anterior and posterior sections, likely consistent with localization of pigmentation (Fig. 5*C*). *Cameo1* expression was relatively uniform.

We examined *CBP* expression by means of quantitative RT-PCR using the same mRNA samples employed for the above experiment. *CBP* expression was definitely repressed in the fourth instar, and increased and peaked in the fifth instar similar to *Cameo2* (Fig. 5*B*). The highest degrees on V2–V4 were consistent with the previous Western blot analysis (13). In the middle silk gland of the *C* allele strain at W0, *CBP* expression was repressed in the anterior section similar to *Cameo2*, but at a high level in the posterior section in contrast to *Cameo2* (Fig. 5*D*).

The C Locus Regulates Cameo2 Expression Likely in a cis-Regulatory Manner—To determine the molecular mechanism by which the *C* locus regulates *Cameo2* expression, we investigated whether the difference of *Cameo2* expression between the *C* and $+^C$ allele is controlled by a *cis*-regulatory element (*i.e.* expression is controlled by a non-coding element such as a

FIGURE 3. **Characteristics of the gene structures of *Cameo1* and *Cameo2*.** *A*, schematic genomic structure. *Connected dotted lines* indicates the structures of the mRNAs. *B*, alignment of putative amino acid sequences of Cameo1 and Cameo2 from the N4 strain. Transmembrane helices predicted by TMHMM version 2.0 (45) are highlighted. *N*-Glycosylation consensus sites (N-*X*-S/T) and cysteine residues in the putative extracellular region, common features in CD36-related genes (64), are indicated by *asterisks* and *bold type*, respectively. The site used to produce the antibody against Cameo2 is indicated by a *dotted underline*. The probable cleavage sites of the signal peptide predicted by the SignalP 3.0-HMM program (46) are indicated by *arrows*. *C*, hypothetical membrane topology of Cameo1, Cameo2, and other homologs predicted by TMHMM version 2.0 and SignalP 3.0-HMM. *D*, the chromosomal locations of the paralogs of *Cameo1* and *Cameo2* in the silkworm. Recently, partial sequences of *Cameo1* and *Cameo2* were reported by data base searches and named *SCRB3* and *SCRB4*, respectively (25). *E*, a neighbor-joining tree for Cameo1, Cameo2, and other homologs from insects and mammals. The first two characters of the gene names represent their species: *Bm*, *B. mori*; *Dm*, *D. melanogaster*; *Ag*, *Anopheles gambiae*; *Hs*, *Homo sapiens*; and *Mm*, *Mus musculus*. Bootstrap values >90%, based on 1000 replicates, are indicated by *closed circles*.

Cameo2 Is Coordinated with CBP in Carotenoid Transport

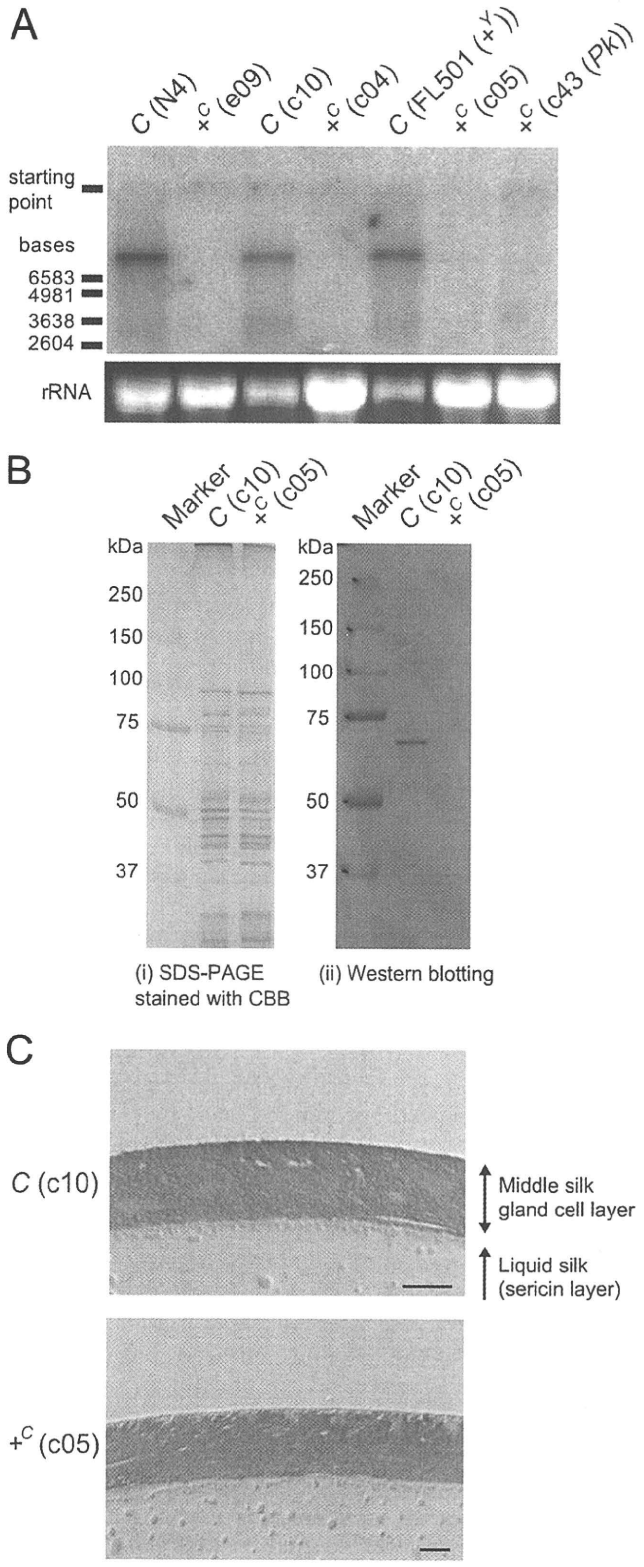

FIGURE 4. **The expression of Cameo2 was definitively repressed in the $+^C$ allele strain.** *A*, Northern blotting analysis of *Cameo2* expression in the middle silk gland at W0. *B*, SDS-PAGE and Western blotting analysis of Cameo2 from the membrane fraction of the middle silk gland at W0. *C*, immunohistochemistry of Cameo2 with the cross-section of the middle silk gland at W0. The *dark red* stains of Cameo2 were found all around the apical surface of the middle silk gland. The *blue stains* are nuclei. *Scale bar*, 20 μm.

transcriptional factor binding site) or a *trans*-acting factor (*i.e.* a coding sequence translated to a protein, such as a transcription factor). We examined SNPs of *Cameo2* mRNA in the middle silk gland of F1 individuals from the cross between the *C* and $+^C$ allele strains. In a *cis*-regulatory mechanism, *Cameo2* would be transcribed dominantly from the chromosome derived from the *C* allele strain (Fig. 6*A*). On the other hand, in a *trans*-acting mechanism, the translated products would act on *Cameo2* genes of both chromosomes from the *C* and $+^C$ allele strains, and *Cameo2* would be transcribed from both chromosomes (Fig. 6*A*). SNP analysis showed that *Cameo2* mRNA was transcribed dominantly from the *C* allele-harboring chromosome in F1 individuals, whereas *Cameo1* mRNA was transcribed from both chromosomes (Fig. 6*B*). Thus, repression of *Cameo2* expression in the $+^C$ allele strain would be controlled by a *cis*-regulatory mechanism.

The C Locus Affects Cameo2 Expression and Carotenoid Accumulation in a Tissue-specific Manner—To examine the tissue specificity of regulation of *Cameo2* expression by the *C* locus, tissue distribution of *Cameo2* was analyzed by Northern blotting (Fig. 6*C*) and RT-PCR (Fig. 6*D*) in the *C* and $+^C$ allele strains. *Cameo2* was expressed in tissues other than the middle silk gland, such as the midgut, testis, ovary, and brain, which was largely unaffected by the *C* gene. As mentioned before, the midgut, testis, and ovary also express CBP in the *Y* allele strain (12, 13). Then, carotenoid pigmentation of the testis and ovary were compared between the *C* and $+^C$ allele strains. In contrast to the difference in the middle silk gland, carotenoid pigmentation of the testis (Fig. 6*E*) and ovary (Fig. 6*F*) were similar between the *C* and $+^C$ allele strains in the background of the *Y* allele. Thus, regulation of *Cameo2* expression and carotenoid accumulation by the *C* locus appeared to be specific for the middle silk gland. Furthermore, carotenoid pigmentation in each tissue seemed to reflect both Cameo2 and CBP expression.

Restoration of Lutein Accumulation by Germ line Transformation with the Cameo2 Gene—To verify the function of Cameo2 as a product of the *C* gene, we examined the restoration of lutein accumulation in the middle silk gland after transgenic expression of the *Cameo2* gene in a strain with the phenotype of yellow hemolymph and white cocoons. The binary *GAL4/UAS* system (30) was used. An effector vector that carried the *Cameo2* gene linked to *UAS* was constructed (Fig. 7*A*) and then the effector UAS-Cameo2 (UAS) lines were generated by germ line transformation. Male moths of a UAS line were crossed with females of the Ser1-GAL4 (GAL4) line that drives target gene expression in the middle silk gland (31). The restoration of pigmentation in the middle silk gland was observed in the GAL4/UAS line (Fig. 7*B*). HPLC analysis of carotenoid content revealed the restoration of selective lutein uptake in the middle silk gland of the GAL4/UAS line (Fig. 7, *C* and *D*). Southern blotting analysis confirmed integration of the *Cameo2* transgene into the UAS line (supplemental Fig. S3*A*). RT-PCR analysis also confirmed an increase in *Cameo2* expression in the middle silk gland of the GAL4/UAS line (supplemental Fig. S3*B*). The GAL4/UAS line produced yellowish colored cocoons, whereas the intensity of coloration was weak (Fig. 7*E*).

Supplemental Material can be found at:
http://www.jbc.org/content/suppl/2010/01/06/M109.074435.DC1.html

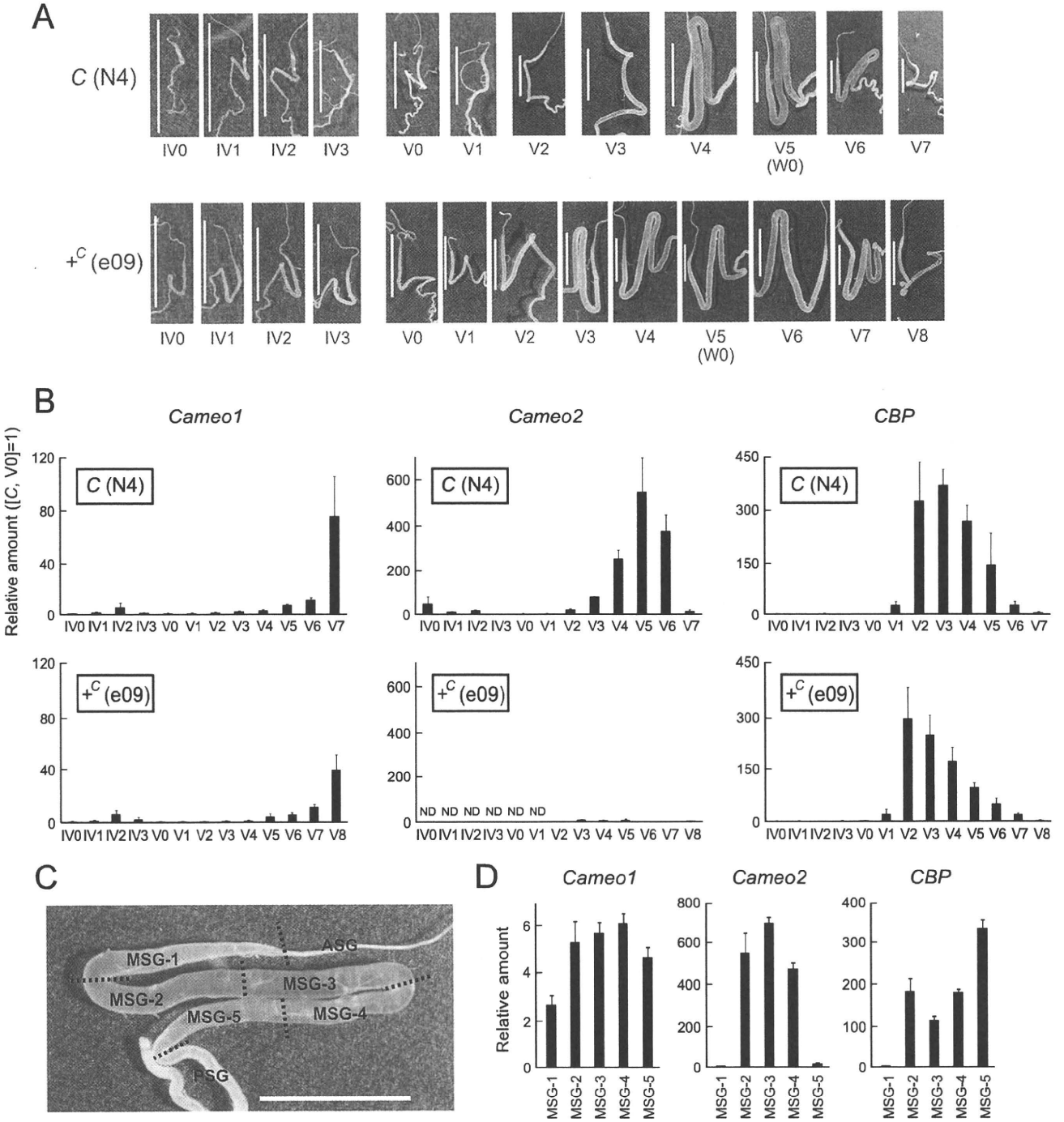

FIGURE 5. **Spatiotemporal analysis of the expression of *Cameo1* and *Cameo2* in the middle silk gland by quantitative RT-PCR.** *A*, changes in carotenoid pigmentation in the silk gland during the fourth and fifth male instars. From V5 (W0), larvae spat silk for cocoon formation, resulting in a decrease of pigmentation in the *C* allele strain. *B*, developmental expression analysis of *Cameo1*, *Cameo2*, and *CBP* in the male middle silk gland. Each *vertical axis* indicates the fold-increase in mRNA expression compared with that of the *C* allele strain at V0 (mean, S.E.; $n = 3$). *ND*, not detected. *C*, cutting lines and definition of regions in the middle silk gland for the expression analysis in *D*. The cutting lines were set at the boundary between the anterior silk gland (*ASG*) and the middle silk gland (*MSG*), the first bend, the midpoint between the first and second bend; the second bend, the midpoint between the second bend and the boundary between the MSG and the posterior silk gland (PSG), and the boundary between the MSG and the PSG. The presented silk gland of the *C* allele strain at the stage of V5 (W0) is the same as in *A*. The pigmentation in MSG-1 can derive from the posterior regions because liquid silk in the core layer of the middle silk gland likely migrates toward ASG (see the less pigmentation in MSG-1 at V4 of the *C* allele strain *A*). *D*, spatial expression analysis of the middle silk gland. Each *vertical* axis indicates the fold-increase in mRNA expression compared with that of the *C* allele strain at V0 as in *B* (mean, S.E.; $n = 3$). The stage was V5 (W0). The same data in *B* and *D* in the logarithmic scale are shown in supplemental Fig. S5. *Scale bar*, 1 cm. *Error bars* are S.E.